

Cosmetic Hydrogen Peroxide Detection Using Nano Bismuth Species Deposited Built-in Three-in-One Screen-Printed Silver Electrode

Mei-Hsin Chiu², Annamalai Senthil Kumar³, Sundaram Sornambikai³, Pei-Yen Chen¹, Ying Shih^{1,*}
and Jyh-Myng Zen^{2,*}

¹ Department of Cosmetic Science Providence University, 200 Chungchi Rd., Taichung 43301, Taiwan.

² Department of Chemistry, National Chung Hsing University, Taichung 402, Taiwan.

³ Environmental and Analytical Chemistry Division, Vellore Institute of Technology University, Vellore-632014, India.

*E-mail: yingshih@pu.edu.tw

Received: 18 May 2011 / Accepted: 11 June 2011 / Published: 1 July 2011

A built-in three-in-one screen-printed electrode assembly containing nano bismuth species deposited silver as working, pre-oxidized silver as reference and unmodified silver as counter electrodes (designated as SPAgE-Bi^{nano}), has been developed for simple electrochemical sensing of H₂O₂ in pH 7 phosphate buffer solution. The working electrode showed ~250 mV reduction in over-potential and a two-fold increased peak current values for electrocatalytic reduction of H₂O₂ over the respective unmodified silver working electrode (i.e. SPAgE) following a diffusion-controlled electron-transfer mechanism. 50 nm sized Bi particles on SPAgE surface was seen in SEM picture of the working electrode. Linear range of H₂O₂ detection from 100 μM to 5 mM, a sensitivity of 0.627 μA /mM and detection limit (S/N = 3) of 56.59 μM were obtained. Finally, SPAgE-Bi^{nano} sensor assembly was utilized for cosmetic H₂O₂ determination, where obtained values and labeled values were in good agreement with recovery in the range of 94.75—101.03 %.

Keywords: Three-in-one screen-printed electrode; silver; Bismuth; hydrogen peroxide; cosmetics.

1. INTRODUCTION

Hydrogen peroxide (H₂O₂) is an important chemical that has wide significance in food, industry, biology, cosmetics, pharmaceutics and environment [1-4]. It is being effectively used as disinfectant, antiseptic, oxidizer and propellant in rocket since many years [5,6]. It can be often found in many day-to-day life cosmetic products such as hair dyes, hair and skin bleaches, conditioners,

shampoos and rinses. For cosmetic human hair bleach, diluted H₂O₂ mixed with ammonium hydroxide solution is used as a constituent [2]. H₂O₂ is also used in tooth whitening products and sold as an antiseptic at concentrations of 3-10% [7]. The Food and Drug Administration (FDA) recommends H₂O₂ as a “substance generally recognized as safe (GRAS)” reagent for food and cosmetic with the recommended concentration limit values of 80 ppm and 6% respectively [8]. Since H₂O₂ is an aggressive oxidizer that can corrode many materials and damage human skin, higher concentration of H₂O₂ (>20%) is considered to be highly hazardous. Hence, simple and sensitive detection of H₂O₂ in commercial real samples is of paramount interest nowadays.

Conventional methods for the detection of H₂O₂ are often based on colorimetric [9-11] and fluorescence [12-14] techniques. Since hydrogen peroxide is lack of chromospheres, it is highly difficult to determine by the conventional techniques without any derivatization procedure. For instance, presence of H₂O₂ is monitored by colorimetry in two steps: (i) oxidizing the iodide to iodine by H₂O₂ in acidic medium and (ii) quantitative bleach of toluidine blue to white by the iodine at 628 nm [11]. Similarly, a fluorescence probe, *para*-hydroxyphenyl acetic acid (HPAA) coupled with *horse radish peroxidase* (HRP) enzyme system was reported for a fluorescence spectroscopy based H₂O₂ quantification assay [12]. Unfortunately, the conventional methods are involved with tedious working procedures and time consuming off-line sample preparations. On the other hand electrochemical technique offers rapid and simple detection methodology for H₂O₂. This technique allows the use of disposable screen-printed electrode (SPE), which has low cost and bulk producible properties and useful for on-site analytical measurements [15]. The purpose of the present study is to establish a simple, sensitive and reliable analytical method for the quantification of hydrogen peroxide in cosmetic products in the physiological/neutral pH, neutral pH is chosen in this case as all the cosmetics are formulated to accommodate with that of the human body condition.

In general, two different electrochemical detection methodologies were reported in literature for H₂O₂, namely; (i) Bio-electrochemical sensor, where HRP [16], *Hemoglobin* [17] and *Cytochrome C* [18] enzyme modified electrodes, and (ii) non-enzyme based approach, in which metal/metal oxides modified electrodes viz., Au [19,20], Pt [21,22], Cu [23-27], Ag [28,29] or molecular complexes such as Prussian Blue [30] and methyl viologen [31] were taken as working electrodes. Considering the cost, stability, reproducibility and enzymeless electrochemical methods, Cu and Ag based electrodes are a better choice for H₂O₂ detection. Nevertheless, since the copper has affinity to form metal complex with some of the cosmetic ingredients, for example, hydroxybenzoate [23] (see section 2.4) and involved in catalytic oxidation of aroma ingredients [25] (perfume), it is not desirable to use copper as a working electrode for the cosmetic real sample analysis. Hence in this work, we are introducing Bi nanoparticles electrodeposited screen-printed silver working electrode (designated as SPAgE-Bi^{nano}) along with in-built counter and reference electrodes as an efficient hydrogen peroxide sensor over silver screen-printed electrode for cosmetic H₂O₂ real sample analysis.

There are many reports on the determination of H₂O₂ from different sources using silver nanoparticles modified conventional electrodes in physiological solution [32-34], however, to the best of our knowledge there are no reports available using metallic silver screen-printed electrode as an underlying substrate. The advantages of using metallic screen-printed electrodes are its mass production capability, flexible SPE designs useful for single users for real time analysis and rapid

detection [35,36]. Further, most of the bulk bismuth modified electrodes are utilized for the anodic stripping voltammetry (ASV) detection of heavy metals, all in acidic medium [37-40]. A Bi modified single crystal gold, Au(111) electrode for the reduction of H₂O₂ says that among different configurations of Bi formed over the electrode surface and only certain configurations are active for catalytic reduction of H₂O₂ [41]. However, the formation of Bi film and the reduction of H₂O₂ are reported in acidic medium in addition to the usage of the expensive gold electrode. Further, preparation of AuSPE is again expensive compared to the above said Cu and Ag based electrodes. Hence in order to reduce the cost of the silver electrode in this work, bismuth metal was modified in the nano form over the SPAgE and to determine the H₂O₂ at a low potential over the corresponding silver electrode, from the cosmetic samples in the physiological solutions with enhanced stability compared to the SPAgE as such.

2. EXPERIMENTAL

2.1. Chemicals and reagents

Hydrogen peroxide (35%), sodium phosphate, sodium phosphate monobasic, phosphoric acid, sodium hydroxide, nitric acid and the bismuth standard solutions were purchased from Sigma (St. Louis, MO. USA) and used as received. Aqueous solutions were prepared using millipore deionized water. Stock solutions of 0.1 M hydrogen peroxide and 100 ppm bismuth were prepared using 0.1 M pH 7 PBS and 0.1 M HNO₃ electrolyte solutions respectively and stored in refrigerator.

2.2. Apparatus and procedure

All the experiments were carried out with a CHI 821b electrochemical workstation (Austin, TX, USA). Preparation of homemade built-in three-in-one screen-printed silver electrode assembly (SPAgE) consists of an Ag-working (a), an Ag/Ag_xO pseudo-reference electrode (b) and an Ag-counter electrode (c), where semi-automatic screen-printer was used to print a conducting silver ink (Acheron, Japan) on a flexible polypropylene film (50 mm × 70 mm) as previously reported [45]. The silver film was cured at 100°C for 10 minutes and then an insulating over layer was printed as a second layer on the silver or carbon printed surface, leaving a working area of diameter 3 mm (0.0707 cm²) along with a counter and a pseudo-reference electrodes as semicircles (Figure 3A). Screen-printed carbon electrode (SPCE) is also prepared by the above procedure, where, instead of the silver, carbon ink (Acheron, Japan) was used. Initial experiments were carried out with SPAgE part as working, conventional Ag/AgCl as reference and 2 mm dia platinum disc as counter electrodes. The pretreatment procedure for the built-in pseudo-reference part (to convert Ag as Ag/Ag_xO) is similar to our earlier report [46]. For the calibration plot and real sample analyses, the built-in three-in-one electrode assembly was directly used. Potential difference between standard Ag/AgCl reference and built-in Ag/Ag_xO pseudo-reference electrode was 350 mV ($E_{\text{pseudoref}} - E_{\text{Ag/AgCl}} = 350 \text{ mV}$). Field emission scanning electron microscopy (FE-SEM) characterization for the working samples, was done

using Carl Zeiss SMT instrument and the X-ray photoelectron spectroscopy (XPS) analysis was carried out using Omicron ESCA spectrometer (Germany) with a monochromatic Al Ka X-ray source. All the XPS spectrum were calibrated with a C 1s standard with binding energy (B.E) value = 284.6 eV. XPS peak fit software program was used for the curve-fitting analysis. Electrochemical experiments were all carried out without deaerating the electrolyte. The H₂O₂ reduction peak current values were measured from the difference between the cathodic peak current values obtained in presence and absence of H₂O₂.

2.3. Preparation of nano Bi modified SPAgE

The SPAgE-Bi^{nano} working electrode was prepared by continuous potential cycling of SPAgE in the window of -0.6 to 0.3 V *versus* Ag/AgCl for twenty cycles ($n=20$) in the presence of 100 ppm bismuth (100 ppm bismuth taken from the 1000 ppm standard Bi solution) containing 0.1 M HNO₃ bath solution (optimal). XPS result given in section 3.1, Figure 2, confirms the formation of Bi^{nano} on the working electrode. After the Bi film formation, the SPAgE-Bi^{nano} is taken out from the deposition bath, washed with copious amount of water and pretreated in 0.1 M pH 7 PBS in the potential window of +0.2 to -0.8 V *versus* Ag/AgCl using cyclic voltammetry (CV) for $n=10$ cycles. Meanwhile, control experiment was also carried out with the deposition of Bi on screen-printed carbon electrode surface (designated as SPE-Bi). Note that the bulk Bi deposition was usually accompanied with non-alloying type electrode surface like carbon with large over-potential for the Bi³⁺ ion deposition [47], while Bi^{nano} is often operated at -0.5 to 0 V *versus* Ag/AgCl on single crystal metallic substrate [48]. For the physicochemical characterization purpose, SPAgE-Bi^{nano} sample, which shows higher current response prepared by potentiostatic polarization method, was taken.

2.4. Cosmetic H₂O₂ real sample analysis

Three cosmetic real samples labeled without (#1) and with (#2 and #3) H₂O₂ were obtained from a local hair salon. Respective % of labeled H₂O₂ values are; 0%, 8.96% and 11.97%. Other ingredient present in the cosmetic samples are: cetylstearyl alcohol, cetrimonium chloride, ceteareth-20, castor oil, methylparaben (Methyl 4-hydroxybenzoate), perfume (aroma compounds), phenacetin (*N*-(4-Ethoxyphenyl)acetamide), phosphoric acid and simethicone (Poly(dimethylsiloxane)). The cosmetic real samples were having the solution pH of ~ 7. In the sample preparation procedure; small amount of real sample was directly mixed with suitable volume of 0.1 M pH 7 PBS and ultrasonicated for 10 min. In the case of samples #1 and #2, 0.25 g of each cosmetic sample was weighed and mixed with 10 mL of 0.1 M pH 7 PBS. 100 μ L of the above solutions were diluted further with 10 mL 0.1 M pH 7 PBS (calculated final dilution factor = 4000). Similarly the sample #3 was prepared by taking 0.1 g of the cosmetic product with a dilution factor of 10000. Standard addition approach was adopted for the real sample analysis, where the real sample combined with standard concentrations of hydrogen peroxide, were taken for the analysis.

3. RESULTS AND DISCUSSION

3.1. Physico-chemical characterizations

The SEM images of unmodified SPAgE (A) and nano Bi modified SPAgE (B and C) designated as SPAgE-Bi^{nano} are shown at different magnifications are given in Figure 1 (Figure 1C is the magnified image of Figure 1B).

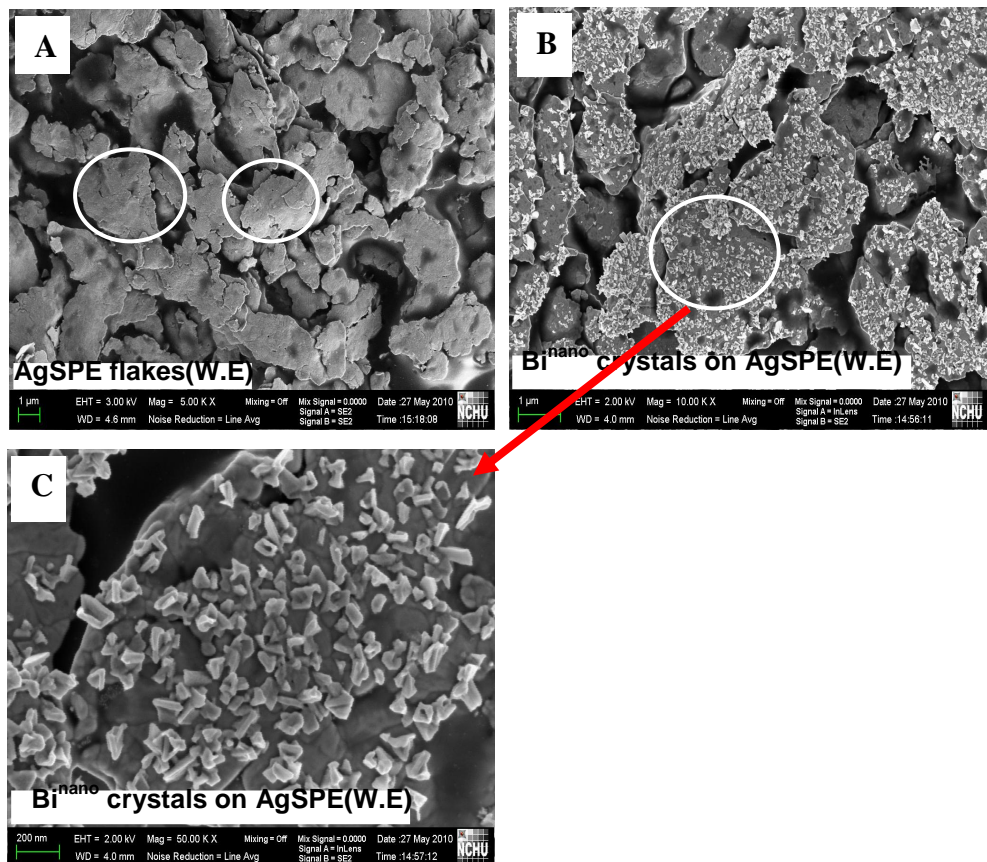


Figure 1. SEM pictures of unmodified SPAgE (A), Bi^{nano} modified SPAgE (B) and magnified image of B (C) at different magnifications. W.E = Working electrode.

The morphology of the SPAgE sample exhibits smooth flakes of approximately 1 μm diameter formed randomly over the underlying substrate with few voids of dimension 0.5 μm. The flake surfaces were nearly smooth. Interestingly, the SEM image of SPAgE-Bi^{nano} showed well defined crystals of 50 nm size on the Ag flakes surface of the SPAgE's electrode. This observation was distinctly different from Bi^{nano} modified carbon electrode, where continuous metallic film of Bi was noticed [42]. The size of the nanoparticles was relatively larger over the Bi^{upd} formed on single crystal gold surface reported earlier [41], where crystallites size was ~1 nm in diameter. Further XPS analysis showed detailed information about the bismuth species formed on the electrode surface.

Figure 2A-D is the comparative XPS responses of SPAgE-Bi^{nano}, SPAgE and SPCE-Bi^{nano} for the Ag 3d and Bi 4f core energy levels. Both the Ag and Bi cores showed doublet peaks corresponding to Ag 3d_{5/2}/3d_{3/2} and Bi 4f_{7/2}/4f_{5/2} energy levels.

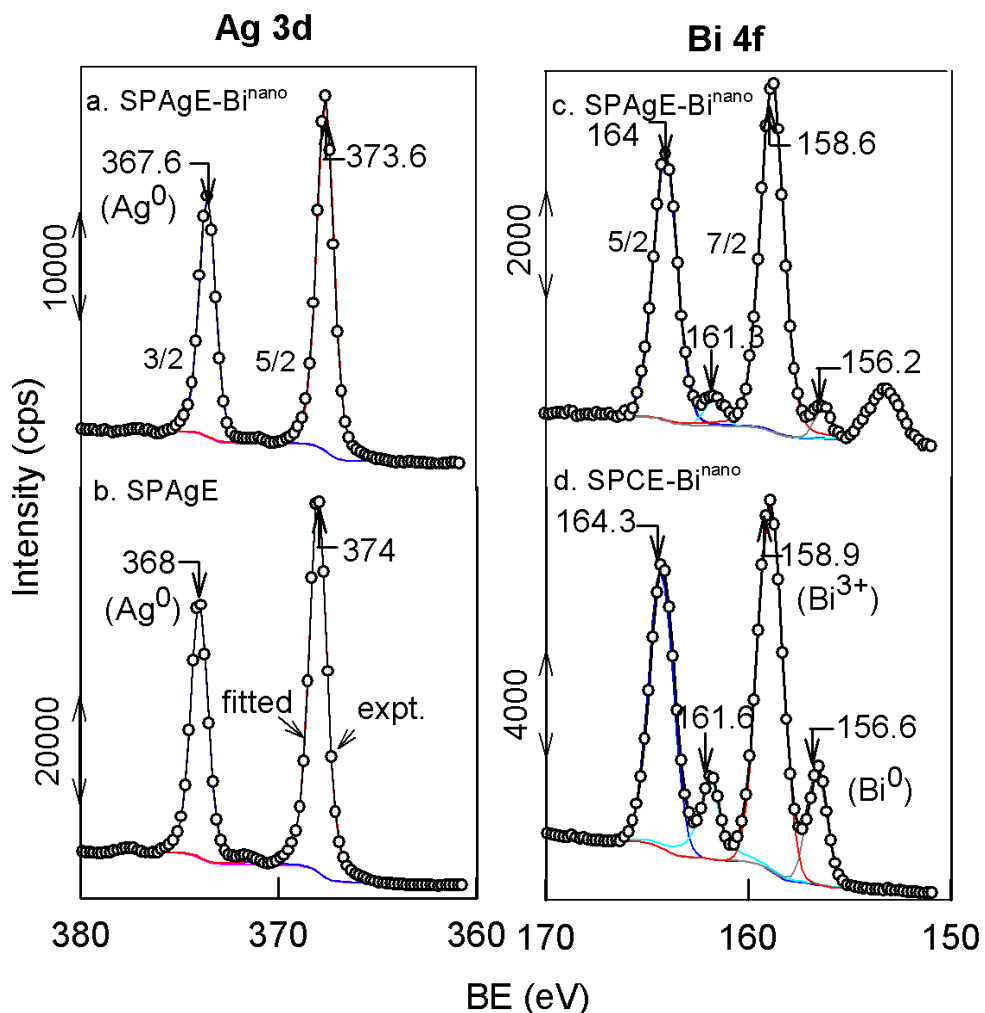


Figure 2. XPS patterns of Ag 3d and Bi 4f core energy levels for various screen-printed silver electrodes.

For the species assignment, the 3d_{5/2} and Bi 4f_{7/2} energy levels were taken as references here. SPAgE and SPAgE-Bi^{nano} samples showed a Ag 3d_{5/2} peak binding energy values at 368 and 367.6 eV respectively, corresponding to a silver metal (Ag⁰) and an alloyed silver-Bi (Ag⁰-Bi) species, correlated to the silver microsphere (368 eV) [43]. The 0.5 eV negative BE shift value observed for the Ag 3d_{5/2} peak after the Bi^{nano} formation, agrees with the literature report [44]. The Bi 4f_{7/2} core energy XPS showed two peaks at BEs 158.9 and 156.6 eV for the SPCE-Bi^{nano} sample, which were in close observation with the BE values of 159.4 and 156.9 eV corresponding to the bulk Bi metal and Bi₂O₃ species for the Bi modified platinum electrode [44]. Calculated Bi^{nano}:B₂O₃ species ratio on the SPCE-Bi^{nano} working surface was 79:21%. In the case of SPAgE-Bi^{nano}, the BE values obtained for Bi

$4f_{7/2}$ are 158.6 and 156.2 eV. Wittstcok et al reported a BE value of 158.7 eV for the atmospheric air exposed Bi^{upd} layer on a polycrystalline Pt surface with a BE of 159 eV, due to BiOOH/Bi(OH)₃ species [44]. These BE values match with our SPAgE-Bi^{nano} electrode and suggests formation of surface confined Bi^{nano} and oxy/hydroxides of bismuth with a % ratio of 95:5 on the screen-printed silver electrode.

3.2. Electro-catalytic H_2O_2 reduction reaction

Figure 3 represents the comparative CV responses of (B) SPCE-Bi^{nano}, (C) SPAgE and (D) SPAgE-Bi^{nano} in absence (dash line) and presence (solid line) of 1 mM H_2O_2 at a scan rate (v) of 50 mV/s, uniformly.

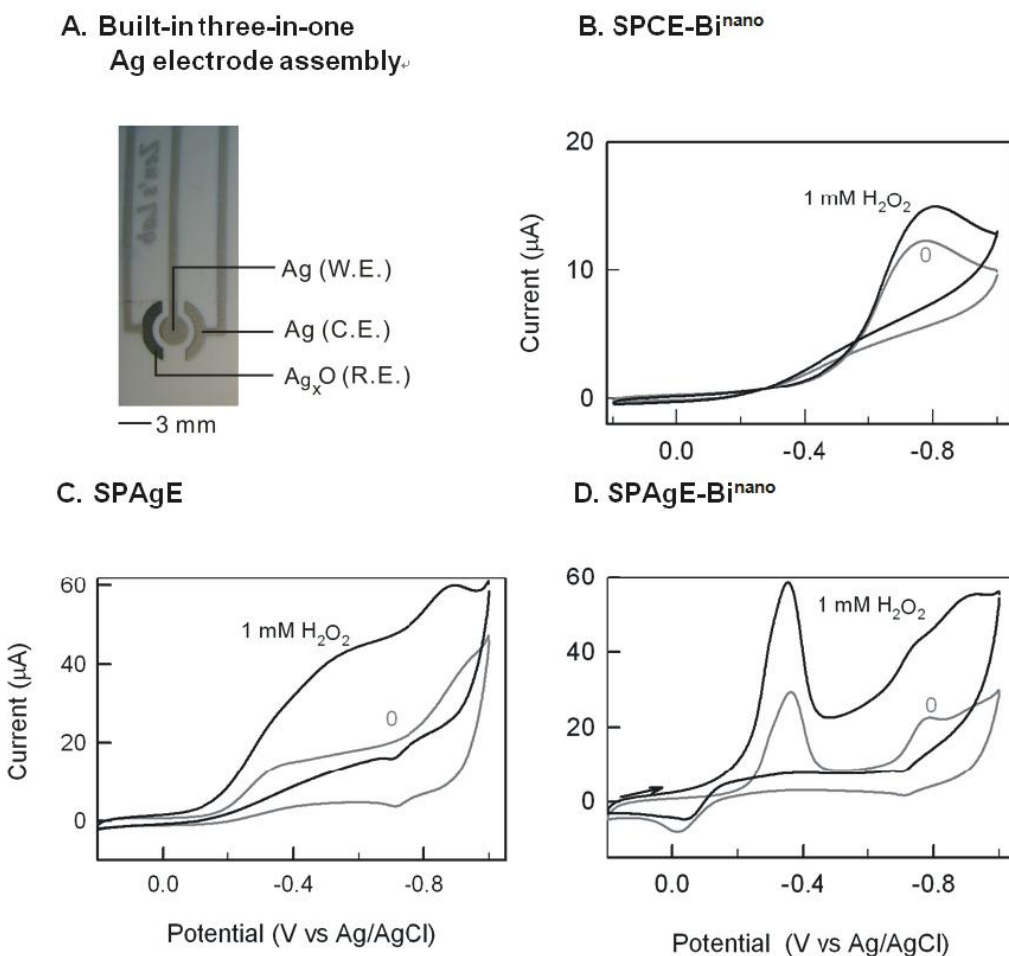


Figure 3. Picture of built-in three-in-one silver screen-printed electrode assembly (A). Comparative CV responses of various screen-printed silver electrodes without and with 1 mM H_2O_2 in pH 7 PBS at a scan rate of 50 mV/s.

All the experiments in this work were done with CV rather than other voltammetry technique, since this is the initial study of utilizing a SPAgE for the determination of H_2O_2 from cosmetic

samples. Exact mechanism for the CV response of the Bi alloy system in this work is unknown for us now. Further work is in progress for extensive mechanism study to extend the findings with advanced quantitative techniques. The SPCE-Bi^{nano} showed highly irreversible reduction peak at -0.8 V *versus* Ag/AgCl which was assigned for the reduction of bulk Bi₂O₃ impurity. The SPCE-Bi^{nano} yields 20% increase in the peak current value in the presence of H₂O₂ without any alteration in the peak potential at -0.8 V. This observation denotes high over-potential for the H₂O₂ reduction reaction on the Bi^{nano} modified electrode. Further, H₂O₂ reduction on unmodified SPAgE showed a shoulder like peak at -0.6 V (Figure 3C). Meanwhile, the bare SPAgE-Bi^{nano} showed feeble anodic peak at 0 V and a sharp counter peak at -0.35 V *versus* Ag/AgCl corresponding to a quasi-reversible behavior of the Bi^{nano} \leftrightarrow Bi₂O₃+3e⁻ reaction [44]. We predict that the peak that appears at 0 V and -0.35 V *versus* Ag/AgCl that was absent in the SPCE-Bi^{nano} may be due to the formation of Ag-Bi alloy.

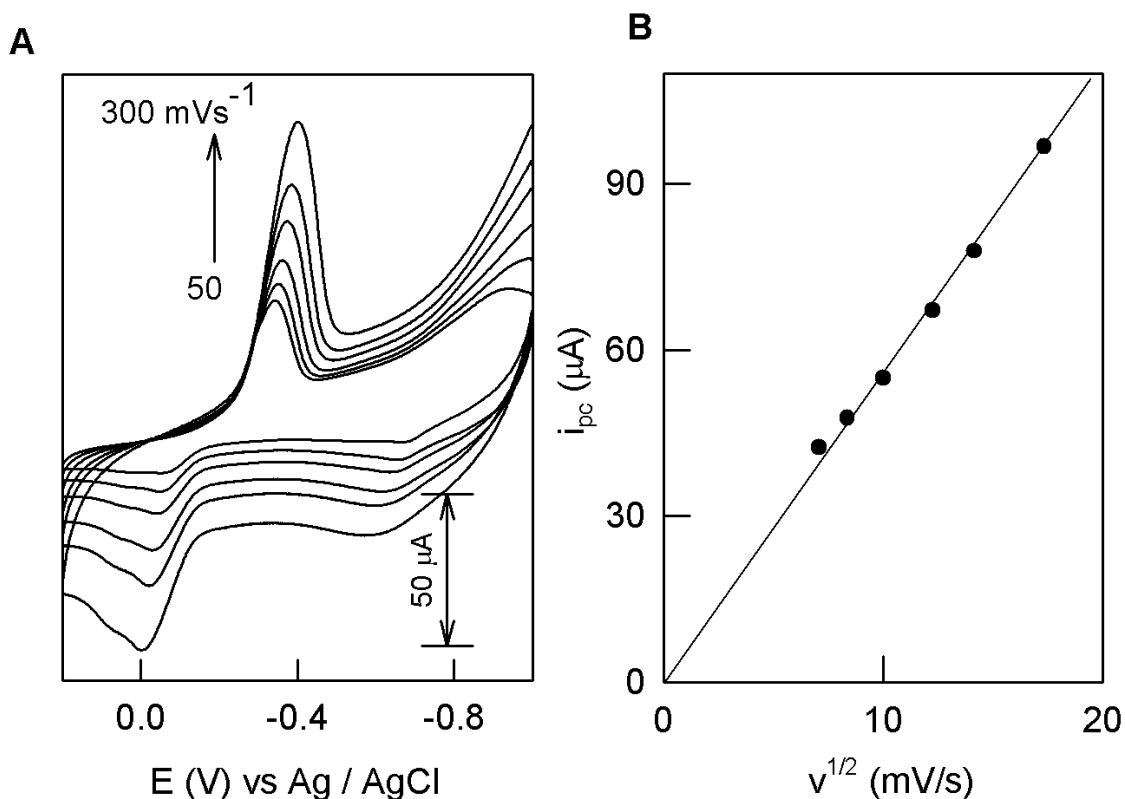


Figure 4. Effect of scan rate on the CV response of SPAgE-Bi^{nano} with 1 mM H₂O₂ in pH 7 PBS (A) and a plot of cathodic peak current (i_{pc}) *versus* square root of scan rate ($v^{1/2}$) (B).

It may also be noted that there are no precise matching report available in the literature for the Bi, its oxide and the alloy of Bi with Ag peaks in the neutral pH. Interestingly, the SPAgE-Bi^{nano} yields two fold increase in the cathodic peak current at -0.35 V over the unmodified electrode (SPAgE) in presence of H₂O₂. Calculated over-potential reduction value was 250 mV. These experimental observations clearly indicate mediated reduction of the H₂O₂ on the bulk screen-printed modified working electrode.

Effect of scan rate for the electro-catalytic H_2O_2 reduction on SPAgE-Bi^{nano} is given in Figure 4A, where systematic increase in cathodic peak current (i_{pc}) against increase in the scan rate was observed. Plot of i_{pc} versus square root of scan rate ($v^{1/2}$), yielded linear line with a slope value of 0.53 (Figure 4B), which is closer the ideal value for the diffusion controlled electron-transfer reaction.

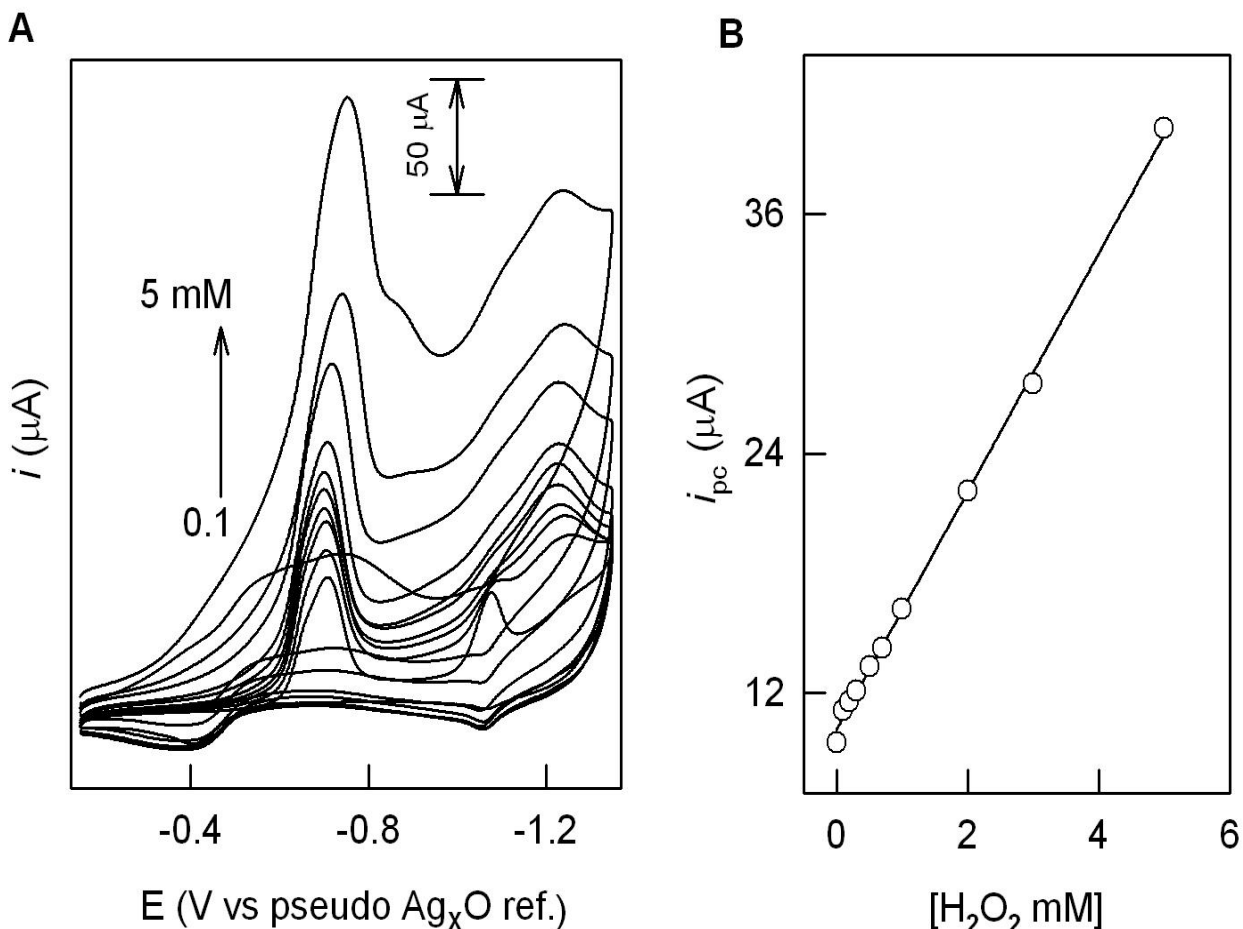


Figure 5. Effect of H_2O_2 concentration on the CV response of SPAgE-Bi^{nano} at a scan rate of 50 mV/s in pH 7 PBS (A) and a plot of peak current, i_{pc} versus H_2O_2 concentration (B).

The effect of H_2O_2 concentration on SPAgE-Bi^{nano} assembly coupled with the built-in Ag/ Ag_xO pseudo-reference electrode as in Figure 5A. Increase in the H_2O_2 concentration starting from 100 μM to 5 mM showed a gradual increase in the reduction peak current values. Constructed calibration plot, base-line corrected peak current (i_{pc}) versus concentration of H_2O_2 ($[\text{H}_2\text{O}_2]$) was linear with a slope and regression coefficient values of 0.627 $\mu\text{A}/\text{mM}$ and 0.9995 respectively. In order to check the reproducibility of the working electrode, the three-in-one electrode assembly was subjected to ten independent CV runs with 0.2 and 0.5 mM of H_2O_2 concentrations repeatedly. Relative standard deviation value (RSD) of 1.2% and 2.7% respectively were obtained (Figure S1), evidences the appreciable reproducibility and stability of the built-in three-in-one screen-printed silver electrode in

this study. Calculated detection limit ($S/N=3$) value was $56.59 \mu\text{M}$, which is comparable to the previous Cu-metal based H_2O_2 detection systems [24,26].

3.3. Real sample analysis

Finally the SPAgE-Bi^{nano} was subjected to H_2O_2 detection in three different cosmetic real samples (#1—#3). Typical CV responses of the real sample #1 and #3 are given in Figure 6A and B respectively. The calibration responses without the real samples (R) were also given for comparison in the figures.

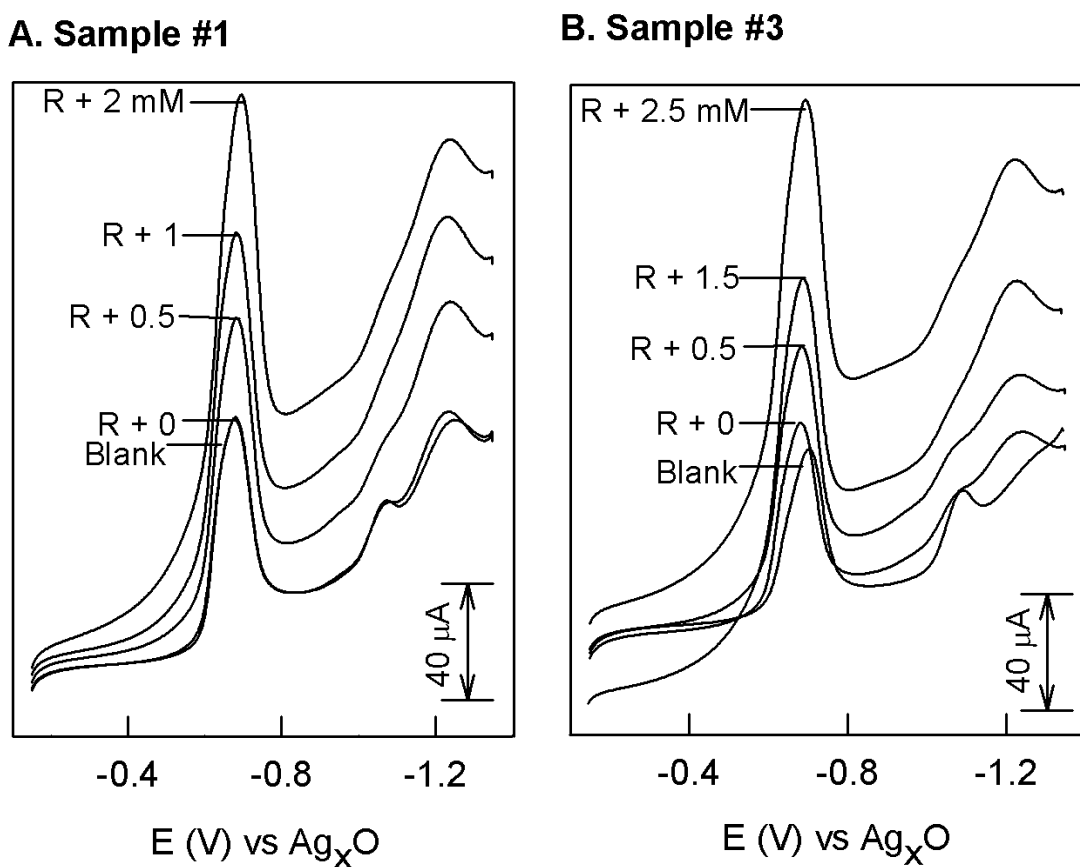


Figure 6. CV responses for the H_2O_2 analysis of cosmetic real samples(R) #1 and #3 on SPAgE-Bi^{nano} as such (blank), without (R) and with (R+N, n=0.5, 1, 1.5, 2, 2.5 mM) known addition of $[\text{H}_2\text{O}_2]$ by standard addition approach. Other working conditions are as in the Figure 5.

As can be seen in Figure 6A, the CV response without and with real sample #1 gave identical peak current values, indicates absence of any H_2O_2 content within the cosmetic formulation, as labeled. On the other hand, upon spiking the real sample #3, specific increase in the peak current on top of the quasi-reversible peak that was obtained for the SPAgE-Bi^{nano} was noticed. Typical standard addition analysis results were shown in the Figure 6A and 6B. Calculated quantitative parameters are tabulated in Table 1. Based on the data, original detected values for the real samples #1—#3 are 0%, 0.95% and

0.49% respectively. After correcting the dilution factors, calculated H₂O₂ content values are 0%, 8.86% and 11.34%, which are in good agreement with the labeled values of 0%, 8.96% and 11.97% respectively for the real samples, revealing that the built-in three-in-one screen-printed electrode assembly proposed in this work is highly efficient for the H₂O₂ detection. Calculated recovery values for the assay were in the window of 94.75—101.03 %, thereby supporting the reliability of the assays for the practical samples (Table 1).

Table 1. Results of the cosmetic H₂O₂ real sample analyses obtained using a built-in SPAgE-Bi^{nano} assembly by cyclic voltammetry in pH 7 PBS.

Sample	Original detected value (mM) ^a	Added (mM)	Found (mM)	Recovery (%)
#1	Nil	0.5	0.500±0.105	100.13±2.10
		1.0	0.998±0.012	99.79±1.24
		2.0	1.933±0.056	96.64±2.79
#2	0.953±0.011	1.0	1.895±0.015	94.75±0.74
		2.0	2.960±0.072	100.35±2.39
		4.0	4.824±0.045	96.49±0.89
#3	0.488±0.009	0.5	0.992±0.023	100.80±2.28
		1.5	2.021±0.060	102.20±2.99
		2.5	2.919±0.043	97.37±1.44

^aDetected value after dilution factor: #1 = 0%, #2 = 8.86 %±0.27, #3 = 11.34 %±0.59
Dilution factors for samples #1 = 4000; #2 = 4000 and #3 = 10,000. Products labeled values are: 1 = 0%, #2 = 8.96 % and #3 = 11.97 %

4. CONCLUSIONS

Bismuth nanoparticles deposited built-in three-in-one screen-printed silver as a working electrode along with screen-printed silver as a reference and a counter electrodes assembly has been demonstrated for the first time for detection of H₂O₂ from cosmetic samples. Scanning electron microscope characterization of the working electrode showed bismuth particles of size ~50 nm on flake like structure of the printed silver. X-ray photoelectron spectroscopic investigation reveals the existence of Bi^{nano} along with BiOOH/Bi₂O₃ species on the working electrode surface. The nano bismuth modified electrode showed efficient electro-catalytic reduction of H₂O₂ with 250 mV reduction in the over-potential compared to the respective unmodified electrode, SPAgE in pH 7 phosphate buffer solution. A diffusion controlled electron transfer mechanism was observed for the H₂O₂ reduction on the working electrode surface with reproducible peak current and a relative standard deviation value of 2.6% (for the 1 mM [H₂O₂]). Finally, H₂O₂ detection assays were successfully demonstrated for three cosmetic real samples using the nano bismuth modified electrode assembly. The

detected and labeled H₂O₂ concentrations were in good agreement. Calculated recovery values for the assays were in the range of 94.75—101.03%. Since, the nano bismuth coated disposable screen-printed silver electrode assembly offers simple detection approach with low cost electrode manufacturing procedures; it can be extendable for various H₂O₂ real samples.

Supplementary data: Plot of peak current *versus* number of runs for the repeated CV detection of 0.5 and 2 mM H₂O₂ detection assays using a SPAgE-Bi^{nano} in pH 7 PBS (Figure S1).

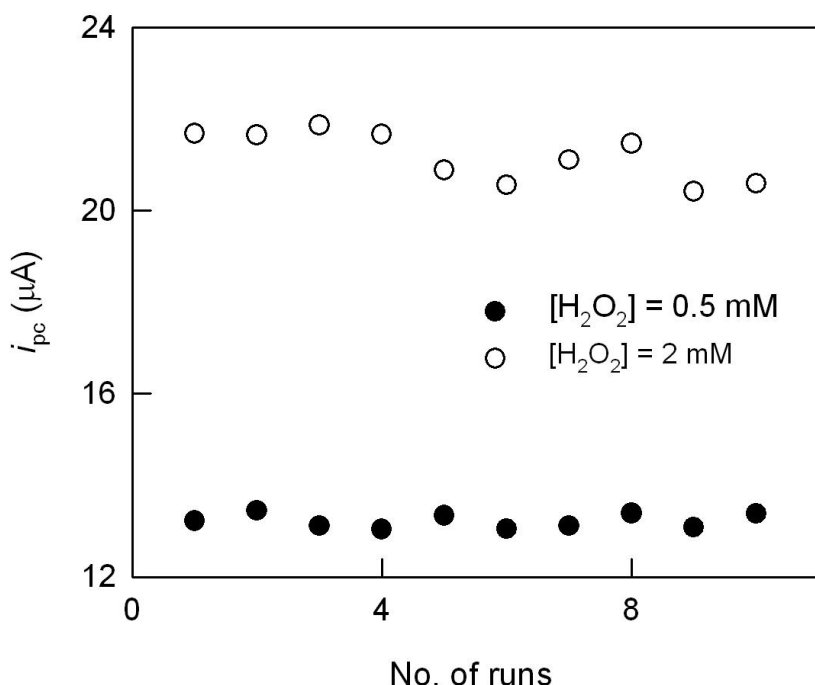


Figure S1. Plot of peak current *versus* number of runs, for the repeated CV of 0.5 and 2 mM H₂O₂ detection using a SPAgE-Bi^{nano} in pH 7 PBS.

ACKNOWLEDGEMENTS

The authors gratefully acknowledge financial supports from the National Science Council of Republic of China (Taiwan).

References

1. O. Demirkol, A.C.-. Mehmetoglu, Z. Qiang, N. Ercal, C. Adams, *J. Agric. Food Chem.*, 56 (2008) 10414.
2. L. Campanella, D. Giancola, E. Gregori, M. Tomassetti, *Sens. Actuator B-Chem.*, 95 (2003) 321.
3. D. Price, P.J. Worsfold, R. Fauzi, C. Mantoura, *TrAC.*, 11 (1992) 379.
4. K. Suzuki, H. Namiki, *Eur. J. Pharmacol.*, 609 (2009) 140.
5. A.P. Silva, C.P.-. Vaz, A.G. Rodrigues, T. Carvalho, *J. Hosp. Infec.*, 76 (2010) P08.05, S23.
6. N. Luo, G.H. Miley, R. Gimlin, R. Burton, *J. Propul. Power.*, 24 (2008) 583.

7. P. Westbroek, J. Hakuzimana, E. Gasana, P. Lombaert, P. Kiekens, *Sens. Actuat. B- Chem.*, 124 (2007) 317.
8. <http://www.fda.gov>
9. B. Zhou, J. Wang, Z. Guo, H. Tan, X. Zhu, *Plant Growth Regul.*, 49 (2006) 113.
10. E. Graf, J.T. Penniston, *Clin. Chem.*, 26/5 (1980) 658.
11. K. Sunil, B. Narayana, *Bull. Environ. Contam. Toxicol.*, 81 (2008) 422.
12. S.S.A.-C. Olina, M. Larstada, G. Ljungkvista, K. Torena, *J. Chromatogr. B.*, 809 (2004) 199.
13. M. Zhou, Z. Diwu, N.P-. Voloshina, R.P. Haugland, *Anal. Biochem.*, 253 (1997) 162.
14. E.K. Paleologos, D.L. Giokas, S.M.T-. Karayanni, M.I. Karayannis, *Anal. Chem.*, 74 (2002) 100.
15. J.-M. Zen, A.S. Kumar, Screen-printed electrochemical sensors, Encyclopedia of sensor, ed. by A.G. Craig, E.C.Elizabeth, V.P. Michael, American Scientific Publishers, California (2006) pp. 33 – 52.
16. J.-L. Huang, Y.-C. Tsai, *Sens. Actuator B- Chem.* 140 (2009) 267.
17. F. Gao, R. Yuan, Y. Chai, M. Tang, S. Cao, *Colloid Suf. A- Physicochem. Eng. Asp.*, 295 (2007) 223.
18. J.-M. Xu, W. Li, Q.-F. Yin, Y.-L. Zhu, *Electrochim. Acta.*, 52 (2007) 3601.
19. J. Xuang, J.L-. Ping, J.-J. Zhu., *Chin. J. Anal. Chem.*, 38 (2010) 513.
20. T.A. Ivandini, R. Sato, Y. Makide, A. Fujishima, Y. Einaga, *Diam. Relat. Mater.*, 14 (2005) 2133.
21. S.B. Hall, E.A. Khudaish, A.L. Hart, *Electrochim. Acta.*, 45 (2000) 3573.
22. A. Kicela, S. Daniele, *Talanta*, 68 (2006) 1632.
23. R.P. Sharma, A. Singh, A. Saini, P. Venugopalan, A. Molinari, V. Ferretti, *J. Mol. Struc.*, 923 (2009) 78.
24. M. Somasundrum, K. Kirtikara, M. Tanticharoen, *Anal. Chim. Acta.*, 319 (1996) 59.
25. H. Nguyen, E.M. Campi, W.R. Jackson, A.F. Patti, *Food Chem.*, 112 (2009) 388.
26. J.-M. Zen, H.-H. Chung, A.S. Kumar, *Analyst*, 125 (2000) 1633.
27. A.S. Kumar, S. Sornambikai, *Ind. J. Chem. Sec-A.*, 48A (2009) 940.
28. C.M. Welch, C.E. Banks, A.O. Simm, R.G. Compton, *Anal. Bioanal. Chem.*, 382 (2005), 12.
29. K. Cui, Y.H. Song, Y. Yao, Z.Z. Huang, L. Wang, *Electrochim. Commun.*, 10 (2008) 663.
30. A.A. Karyakin, *Electroanalysis*, 13 (2001) 813.
31. J.-M. Zen, S.H. Jeng, H.J. Chen, *J. Electroanal. Chem.*, 408 (1996) 157.
32. S. Wu, H. Zhao, H. Ju, C. Shi, J. Zhao., *Electrochim. Commun.*, 8 (2006) 1197.
33. W. Lian, L. Wang, Y. Song, H. Yuan, S. Zhao, P. Li, L. Chen, *Electrochim. Acta.*, 54 (2009) 4334.
34. A. Safavi, N. Maleki, E. Farjam, *Electroanalysis*, 21 (2009) 1533.
35. J. Wang, *Acc. Chem. Res.*, 35 (2002) 811.
36. M.-H. Chiu, J.-M. Zen, A.S. Kumar, D. Vasu, Y. Shih, *Electroanalysis*, 20 (2008) 2265.
37. C. Kokkino, A. Economou, I. Raptis, C.E. Efstatithiou, T. Speliotis, *Electrochim. Commun.*, 9 (2007) 2795.
38. Z. Zou, A. Jang, E. MacKnight, P-M. Wu, J. Doa, P.L. Bishop, C.H. Ahn, *Sens. Actuat. B.*, 134 (2008) 18.
39. L. Baldrianova, I. Svancara, M. Vlcek, A. Economou, S. Sotiropoulos, *Electrochim. Acta.*, 52 (2006) 481.
40. S.M. Skogvold, O. Mikkelsen, *Electroanalysis*, 20 (2008) 1738.
41. M. Nakamura, N. Sato, N. Hoshi, O. Sakata, *Langmuir*, 26 (2010) 4590.
42. E. Sandnes, M.E. Williams, U. Bertocci, M.D. Vaudin, G.R. Stafford, *Electrochim. Acta.*, 52 (2007) 6221.
43. B. Zhao, Z. Liu, Z. Liu, G. Liu, Z. Li, J. Wang, X. Dong, *Electrochim. Commun.*, 11 (2009) 1707.
44. G. Wittstock, A. Strubing, R. Szargan, G. Werner, *J. Electroanal. Chem.*, 444 (1998) 61.
45. J.-M. Zen, C.-C. Yang, A.S. Kumar, *Electrochim. Acta.*, 47 (2001) 899.
46. M.-H. Chiu, W.-L. Cheng, G. Muthuraman, C.-T. Hsu, H.-H. Chung, J.-M. Zen., *Biosensor. Bioelectron.*, 24 (2009) 3008.

47. E.A. Hutton, B. Ogorevc, S.B. Hoevar, F. Weldon, M.R. Smyth, J. Wang, *Electrochim. Commun.*, 3 (2001) 707.
48. Y.-C. Fu, Y.-Z. Su, H.-M. Zhang, J.-W. Yan, Z.-X. Xie, B.-W. Mao., *Electrochim. Acta.*, 55 (2010) 8105.